Utilizing belief functions for the estimation of future climate change

Elmar Kriegler*, Hermann Held†

Potsdam Institute for Climate Impact Research, Telegrafenberg, 14473 Potsdam, Germany

ABSTRACT

We apply belief functions to an analysis of future climate change. It is shown that the lower envelope of a set of probabilities bounded by cumulative probability distributions is a belief function. The large uncertainty about natural and socio-economic factors influencing estimates of future climate change is quantified in terms of bounds on cumulative probability. This information is used to construct a belief function for a simple climate change model, which then is projected onto an estimate of global mean warming in the 21st century. Results show that warming estimates on this basis can generate very imprecise uncertainty models.

Keywords: climate change, climate sensitivity, imprecise probability, belief function, random set, probability box, distribution band

1. Introduction

It is widely accepted that a discernible influence of industrial and agricultural emissions of greenhouse gases (GHGs) on the earth's climate exists. Due to human activity, greenhouse gas concentrations in the atmosphere have risen by, to name just a few gases, 35% for carbon dioxide, 250% for methane and 15% for nitrous oxide. Empirical evidence for a growing climate change signal is mounting, and all state-of-the-art climate models

*Corresponding author: kriegler@pik-potsdam.de
†held@pik-potsdam.de

need the increased absorption of infrared radiation from the earth surface due to growing GHG concentrations to reproduce this signal. Still, uncertainty abounds. How sensitive is the climate to growing GHG concentrations? What amount of greenhouse gases will humankind put into the atmosphere in the 21st century?

We believe that the application of imprecise probability concepts carries the potential to greatly improve the situation in climate change forecasting and integrated assessment of climate change policies. However, an obstacle might be the dynamical nature of climate change models, and the large number of uncertain variables which mostly range over continuous possibility spaces. In this paper, we present an application of belief functions to the estimation of global mean temperature (GMT) change in the 21st century. Belief functions have been widely used with varying interpretations. Luo and Caselton [1], for example, have presented an early application of belief functions to climate change by drawing on Dempster's theory [2] which builds on a basic probability assignment to sets.

We interpret a belief function as lower envelope of a set of probability measures, and try to respect this interpretation throughout the reasoning process. The uncertainty on the climate model parameters is initially quantified by lower and upper cumulative probability distribution functions (CDFs) on the real line. In Section 2, we discuss how this information can be converted to a belief function, combined for different model parameters, and projected onto the model output. In Section 3, we present the simple temperature change model, and construct a joint belief function for its uncertain parameters. In Section 4, the uncertainty in the input values is projected onto an estimate of global mean temperature change. Section 5 concludes the paper. To enhance readability, proofs of formal statements are delegated to the Appendix.

2. Methods

2.1. Basic Concepts

We briefly introduce the basic concepts that are used throughout the paper. Consider an uncertain quantity X that enters a model of some causal relationship, e.g., of the link between GHG emissions and GMT. The uncertainty about X shall be described by a lower bounding function $\underline{F}_X : \mathbb{R} \to [0,1]$ and an upper bounding function $\overline{F}_X : \mathbb{R} \to [0,1]$ for a set of CDFs $F_X(x) := P(X \leq x)$ on the real line $\mathbb{R}$. The resulting set of probabilities

$$\Gamma_X(\underline{F}, \overline{F}) := \{\, P \,|\, \forall\, x \in \mathbb{R} \quad \underline{F}(x) \leq P(-\infty, x] \leq \overline{F}(x) \,\} \tag{1}$$

has been called a *distribution band* in the literature [3]. Γ_X is convex, since for any two probabilities $P, Q \in \Gamma_X$ and $\lambda \in (0,1)$, also $\lambda P + (1-\lambda)Q \in \Gamma_X$.

If the lower and upper bounding functions are continuous on the real line, we call Γ_X a *continuous distribution band*. Another important special case is constituted by lower and upper step functions $\underline{SF}$, $\overline{SF} : \mathbb{R} \to \{0, a_1, ..., a_n, 1\}$. The resulting convex set of probabilities $\Gamma_X(\underline{SF}, \overline{SF})$ is called a *probability box (p-box)* [4]. P-boxes naturally emerge, when the distribution of a continuous random variable on the real line is approximated by lower and upper step functions $\underline{SF} \leq F \leq \overline{SF}$, where $F \leq \overline{SF}$ denotes pointwise domination. Such an approximation was employed to calculate bounds for the convolution of two random variables with unknown dependency [5].

Likewise, a continuous distribution band $\Gamma_X(\underline{F}, \overline{F})$ with bounded support can be enclosed by a p-box $\Gamma_X(\underline{SF}, \overline{SF}) \supset \Gamma_X(\underline{F}, \overline{F})$[1]. The smallest such p-box is bounded by a right-continuous step function $\underline{SF} \leq \underline{F}$ from below and a left-continuous step function $\overline{SF} \geq \overline{F}$ from above (see Fig. 1). Right- and left-continuity of the bounds are necessary conditions for the p-box to be the smallest discrete approximation that encompasses the continuous distribution band.

In the following, we focus our discussion on p-boxes $\Gamma_X(\underline{SF}, \overline{SF})$ with right- and left-continuous bounding functions. Our goal is to identify a simple uncertainty representation for these p-boxes, which fully captures their information content. The information content of a convex set of probabilities can sometimes, but not always, be assessed in terms of its *lower envelope* $\underline{P} : \mathcal{A} \to [0,1]$ on the domain $\mathcal{A}$ of measurable events. A natural choice of domain for real-valued random variables X is the Borel field $\mathcal{R}$ of $\mathbb{R}$ [6, Sect. 14]. Then, the lower envelope $\underline{P}_X$ of a p-box $\Gamma_X(\underline{SF}, \overline{SF})$ is defined by

$$\forall\, A \in \mathcal{R} \quad \underline{P}_X(A) := \inf_{P \in \Gamma_X(\underline{SF}, \overline{SF})} P(A)\ . \tag{2}$$

In Section 2.2, it will be shown that the lower envelope $\underline{P}_X$ of $\Gamma_X(\underline{SF}, \overline{SF})$ is a *belief function*. Belief functions have been introduced by Dempster [2] and further explored by Shafer [7]. They are defined as totally monotone set functions $bel : \mathcal{A} \to [0,1]$, i.e., for an arbitrary countable union of sets $\mathrm{A}_i \in \mathcal{A}$ indexed by $I = \{1, 2, ...\}$,

$$bel\left(\cup_{i \in I}\, A_i\right) \geq \sum_{J \subseteq I,\ J \neq \emptyset} (-1)^{|J|+1}\ bel(\cap_{j \in J} A_j)\ .$$

[1] If the support of $\Gamma_X(\underline{F}, \overline{F})$ is not bounded, a step function approximation with bounded support will cut the tails of the distribution band. Any further analysis with $\Gamma_X(\underline{SF}, \overline{SF})$ will disregard the information contained in these tails. This can be critical, e.g., when observations are used to correct prior knowledge. P-boxes with unbounded support might be used, but their discussion is beyond the scope of this paper.

In the special case of equality between the left- and right-hand side, *bel* is a probability measure. Belief functions have favorable properties. In particular, their *Möbius inverse* $m : \mathcal{A} \to \mathbb{R}$, defined by $\forall\, A \in \mathcal{A}\ \ bel(A) = \sum_{B \subseteq A} m(B)$, exhibits only non-negative entries $m(B) \geq 0$ which sum up to unity, i.e., $\sum_{A \in \mathcal{A}} m(A) = 1$ [2, 7]. Thus, $m : \mathcal{A} \to \mathbb{R}$ can be interpreted as a *basic probability assignment* on $\mathcal{A}$. The sets $A \in \mathcal{A}$ with $m(A) > 0$ are called *focal elements*. In this paper, we only consider belief functions with a finite number of focal elements. Let $\mathcal{E} = \{E_1, ..., E_n\}$ be the collection of focal elements. The tuple $(\mathcal{E}, m) := \{(E_1, m(E_1)), ..., (E_n, m(E_n))\}$ is called a (finite support) *random set* or *focal set*. Knowledge of the random set $(\mathcal{E}, m)$ suffices to determine *bel* and its conjugate set function *pl*, called *plausibility function*, which is defined by $\forall\, A \in \mathcal{A}\ \ pl(A) = 1 - bel(A^c)$. It is

$$bel(A) = \sum_{B \subseteq A} m(B) \ = \sum_{i \,|\, E_i \subseteq A} m_i\,, \quad pl(A) = \sum_{B \cap A \neq \emptyset} m(B) \ = \sum_{i \,|\, E_i \cap A \neq \emptyset} m_i\,.$$

2.2. Representing P-Boxes by Belief Functions

It was already noted by Yager [8] that p-boxes $\Gamma_X(\underline{SF}, \overline{SF})$ exhibit a close relationship to belief functions. In the following, we will further explore this relationship. It is assumed that the bounding step functions have the form

$$\underline{SF}(x) = \begin{cases} \underline{SF}(x_{*i}) & x_{*i} \leq x \\ & \quad < x_{*i+1} \\ 0 & x < x_{*1} \\ 1 & x_{*n} \leq x \end{cases}, \ \overline{SF}(x) = \begin{cases} \overline{SF}(x^*_{j+1}) & x^*_j < x \\ & \quad \leq x^*_{j+1} \\ 0 & x \leq x^*_1 \\ 1 & x^*_m < x \end{cases}.$$

The following algorithm can be used to construct a random set $(\mathcal{E}, m)$ from $\underline{SF}$ and $\overline{SF}$ (see Fig. 1).

ALGORITHM 1. **1.** *Initialize indices $k = 1$ (running over the focal elements of the random set to be constructed), $i = 1$ (running over x_{*i}), $j = 1$ (running over x^*_j). Let p_k denote the cumulative probability already accounted for in step k. Assign $p_0 = 0$.*

2. *Construct focal element $E_k = (x^*_j,\, x_{*i}]$.*

3. *If $j = m$, choose arbitrary $x^*_{m+1} > x^*_m$, thus $\overline{SF}(x^*_{m+1}) = 1$.*

(a) *$\underline{SF}(x_{*i}) < \overline{SF}(x^*_{j+1})$: $m_k = \underline{SF}(x_{*i}) - p_{k-1}$, $p_k = \underline{SF}(x_{*i})$. Raise indices $k \to k+1$, $i \to i+1$. Return to Step 2.*

(b) *$\underline{SF}(x_{*i}) > \overline{SF}(x^*_{j+1})$: $m_k = \overline{SF}(x^*_{j+1}) - p_{k-1}$, $p_k = \overline{SF}(x^*_{j+1})$. Raise indices $k \to k+1$, $j \to j+1$. Return to Step 2.*

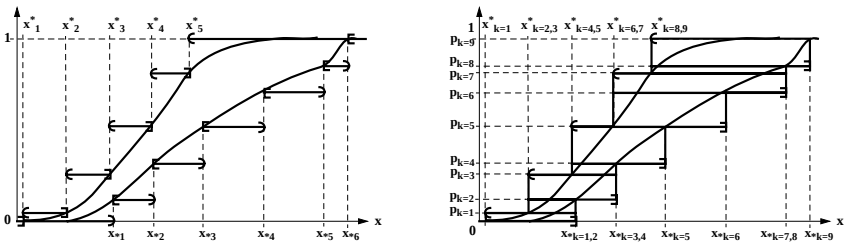

Figure 1. Illustration of the p-box approximation of a distribution band (left panel), and the construction of a random set from a p-box by use of Algorithm 1 (right panel).

(c) $\underline{SF}(x_{*i}) = \overline{SF}(x^*_{j+1})$: $\quad m_k = \overline{SF}(x^*_{j+1}) - p_{k-1}$.
If $\underline{SF}(x_{*i}) = \overline{SF}(x^*_{j+1}) = 1$, *stop.*
If $\underline{SF}(x_{*i}) = \overline{SF}(x^*_{j+1}) < 1$, *set* $p_k = \overline{SF}(x^*_{j+1})$. *Raise indices* $k \to k+1$, $i \to i+1$, $j \to j+1$. *Return to Step 2.*

For each step k, it is $x^*_j \leq x_{*i}$ (since $\overline{SF} \geq \underline{SF}$), and $m_k > 0$ (since $\overline{SF}$, $\underline{SF}$ monotone increasing). The algorithm will always reach the points x_{*n}, x^*_{m+1} with $\underline{SF}(x_{*n}) = \overline{SF}(x^*_{m+1}) = 1$ and stop.

LEMMA 1. *Algorithm 1 constructs a random set* $(\mathcal{E}, m)$, *which has the following properties:*

(I) $(\mathcal{E}, m)$ *contains* $q < n+m$ *half-closed intervals* $E_k = (x^*_{j(k)}, x_{*i(k)}]$ *as focal elements.*

(II) $(\mathcal{E}, m)$ *includes no pair of focal elements* E_k, E_l *with* $x^*_{j(k)} < x^*_{j(l)} < x_{*i(l)} < x_{*i(k)}$.

(III) $\forall\, x \in \mathbb{R}$, *the associated belief and plausibility functions fulfill* $bel_{\mathcal{E}}(-\infty, x] = \underline{SF}(x)$, $pl_{\mathcal{E}}(-\infty, x] = \overline{SF}(x)$.

Similar algorithms have been presented in the literature [4, 9]. The main difference is constituted by the fact that Algorithm 1 generates half-closed intervals $E_k = (x^*_k, x_{*k}]$, while other formulations usually choose the corresponding closed interval $\tilde{E}_k = [x^*_k, x_{*k}]$. Since for all k $E_k \subset \tilde{E}_k$, $bel_{\mathcal{E}} > bel_{\tilde{\mathcal{E}}}$ and $pl_{\mathcal{E}} < pl_{\tilde{\mathcal{E}}}$ for some sets in $\mathcal{R}$. Consider, e.g., the set $(-\infty, x^*_l]$. Due to property (II), $pl_{\mathcal{E}}(-\infty, x^*_l] = \sum_{k<l} m_k < \sum_{k \leq l} m_k = pl_{\tilde{\mathcal{E}}}(-\infty, x^*_l]$. Since $pl_{\mathcal{E}}(-\infty, x^*_l] = \overline{SF}(x^*_l)$, the choice of closed intervals instead of half-closed intervals leads to $pl_{\tilde{\mathcal{E}}}(-\infty, x] > \overline{SF}(x)$ at the points $x = \{x^*_1, ..., x^*_q\}$. For application purposes, this additional imprecision does not matter much, since $pl_{\tilde{\mathcal{E}}}(-\infty, x]$ and $\overline{SF}(x)$ agree almost everywhere on the real line. However, if we want to show that the information content of a p-box $\Gamma_X(\underline{SF}, \overline{SF})$ is completely captured by the random set constructed from Algorithm 1, we need to be more precise.

THEOREM 1. *Let $\Gamma_X(\underline{SF}, \overline{SF})$ be a p-box on the real line bounded by a left-continuous step function $\overline{SF} : \mathbb{R} \to [0,1]$ from above and a right-continuous step function $\underline{SF} : \mathbb{R} \to [0,1]$ from below (see Definition 1).*

Let $\underline{P}_X : \mathcal{R} \to [0,1]$ be the lower envelope of Γ_X on the Borel field $\mathcal{R}$ as defined in Equation (2).

Let $(\mathcal{E}, m)$ be the random set constructed from $\underline{SF}$ and $\overline{SF}$ by Algorithm 1, and $bel_{\mathcal{E}} : \mathcal{R} \to [0,1]$ the associated belief function.

Then, $\forall\, A \in \mathcal{R} \quad bel_{\mathcal{E}}(A) = \underline{P}_X(A)$.

As a direct consequence of Theorem 1, the p-box $\Gamma_X(\underline{SF}, \overline{SF})$ coincides with the convex set of probabilities $\Gamma_X(bel_{\mathcal{E}}) := \{\, P \,|\, \forall\, A \in \mathcal{R} \quad bel_{\mathcal{E}}(A) \leq P(A) \,\}$ that is encompassed by the belief function $bel_{\mathcal{E}}$. This can be seen by noting that every $P_X \in \Gamma_X(bel_{\mathcal{E}})$ has to be an element of $\Gamma_X(\underline{SF}, \overline{SF})$, since $\forall\, x \in \mathbb{R}$ it is $bel(-\infty, x] := \underline{SF}(x) \leq P_X(-\infty, x] \leq pl(-\infty, x] := \overline{SF}(x)$. In turn, every $P_X \in \Gamma_X(\underline{SF}, \overline{SF})$ has to be an element of $\Gamma_X(bel_{\mathcal{E}})$, since $bel_{\mathcal{E}}$ is the lower envelope of $\Gamma_X(\underline{SF}, \overline{SF})$.

Thus, the p-box $\Gamma_X(\underline{SF}, \overline{SF})$ can be represented indeed by a belief function $bel_{\mathcal{E}}$. However, not every $bel_{\mathcal{E}}$ constitutes a p-box. The following corollary of Theorem 1 establishes necessary and sufficient conditions for $bel_{\mathcal{E}}$ to be the representation of a p-box.

COROLLARY 1. *Let $bel_{\mathcal{E}} : \mathcal{R} \to [0,1]$ be a belief function with (finite support) random set $(\mathcal{E}, m)$, which defines a right-continuous $\underline{SF} : \mathbb{R} \to [0,1]$ and left-continuous $\overline{SF} : \mathbb{R} \to [0,1]$ by $\underline{SF}(x) := bel(-\infty, x]$ and $\overline{SF}(x) := pl(-\infty, x] = 1 - bel(x, +\infty)$ for all $x \in \mathbb{R}$. Then,*

$$\Gamma_X(bel_{\mathcal{E}}) \subseteq \Gamma_X(\underline{SF}, \overline{SF}) \,,$$

where equality holds if and only if $(\mathcal{E}, m)$ has Properties (I) and (II) in Lemma 1.

2.3. Combining Belief Functions

In almost all assessments of climate change, uncertainty accumulates from different sources. Thus, we wish to consider a multivariate uncertainty model with uncertain quantities $X = \{X_1, ..., X_n\}$, each of which is described by a p-box $\Gamma_{X_i}(\underline{SF}, \overline{SF})$ on the real line. If the uncertain quantities X_i were independent and described by marginal probability measures P_{X_i}, there would exist a unique way to construct a product measure P_X. If they are described by belief functions constituting the lower envelopes of the p-boxes, however, the situation is more complicated. For non-additive lower probabilities like belief functions, the joint lower envelope $\underline{P}_X$ of

the independent product depends on the concept of independence that is considered [10, 11].

Assume that the uncertainty about the quantities X_i is represented by belief functions bel_{X_i} with associated random sets $(\mathcal{E}_i, m_i) = \{(E_{1_i}, m_{1_i}),$ ..., $(E_{k_i}, m_{k_i})\}$, $1 \leq i \leq n$. There exists a simple way to construct the Möbius inverse of a particular choice of independent product bel_X from the Möbius inverses of the bel_{X_i} [2]. It is expressed in terms of a joint random set $(\mathcal{E}, m)$, which is calculated from the marginal random sets $(\mathcal{E}_i, m_i)$ by

$$(\mathcal{E}, m) := \{ (E_{l_1 \ldots l_n} = E_{l_1} \times \ldots \times E_{l_n}, m_{l_1 \ldots l_n} = m_{l_1} \cdot \ldots \cdot m_{l_n}),\ 1 \leq l_i \leq k_i \}\,. \quad (3)$$

The independence concept associated with Definition (3) has been called *random set independence* in the literature. Using the example of random draws from two urns with unknown proportions of red and white balls, Couso et al. [10] have compared random set independence with other concepts of independence for convex sets of probabilities, in particular with epistemic and strong independence [11, Ch. 9.3]. Their comparison indicated that random set independence yields weaker information than other independence concepts. Recently, Fetz and Oberguggenberger [12] and de Cooman [13] showed that the convex set of joint probabilities encompassed by the random set independent lower envelope constitutes always a superset of the probabilities that are encompassed by the epistemic and strong independent lower envelope, respectively. Random set independence yields the most conservative estimate of the joint uncertainty that can be obtained under an independence assumption.

It was pointed out by Regan et al. [9], that random set independence can be extended to the case of belief functions with unknown dependency by drawing on the equivalence of random sets to *thickets*. Thickets are employed in the Distribution Envelope Determination (DEnv) method [14]. DEnv uses linear programming to compute a lower and upper bound on the probability assignment m_{A*B} for the combination of two intervals $A * B$ from the probability assignments m_A and m_B [14]. See also Fetz and Oberguggenberger [12] for an alternative discussion of combining random sets with unknown dependency.

Consider the special case of two marginal random sets $(\mathcal{E}_1, m_1) = \{(E_{1,1}, m_{1,1}),$ ..., $(E_{1,n}, m_{1,n})\}$ on Ω_X and $(\mathcal{E}_2, m_2) = \{(E_{1,1}, m_{1,1}),$ ..., $(E_{2,k}, m_{2,k})\}$ on Ω_Y, where no pair of focal elements is nested. This condition, albeit not fully enforced by property (II) in Lemma 1, is frequently fulfilled when approximating a distribution band $\Gamma_X(\underline{F}, \overline{F})$ with a p-box $\Gamma_X(\underline{SF}, \overline{SF})$, and constructing the associated random set (see section 3.1). The conjunction of two events $E_{1,i} \times \Omega_Y$ and $\Omega_X \times E_{2,i}$ of unknown dependency with lower probabilities $\underline{P}(E_{1,i}) = m_{1,i}$ and $\underline{P}(E_{2,j}) = m_{2,j}$ yields a lower and upper Fréchet bound for the probability of the joint event

$E_{ij} = E_{1,i} \times E_{2,j}$:

$$\underline{P}(E_{ij}) := m_{ij} \geq \max[0, m_{1,i} + m_{2,i} - 1] \ , \tag{4}$$

$$\overline{P}(E_{ij}) := \sum_{lm|E_{lm}\cap E_{ij}\neq\emptyset} m_{lm} \leq \min[\sum_{l|E_{1,l}\cap E_{1,i}\neq\emptyset} m_{1,l}, \sum_{m|E_{1,m}\cap E_{2,j}\neq\emptyset} m_{2,m}] \, . \tag{5}$$

For an arbitrary event $A \subset \Omega_X \times \Omega_Y$, Constraints (4) and (5) define a linear programming problem for finding the probability mass assignment m_{1*2} over the joint random set $(\mathcal{E}_1 \times \mathcal{E}_2, m_{1*2})$ that minimizes $bel_{1*2}(A)$. Thus, the independent product (3) for the case of independent marginals can be generalized to the case of marginals with unknown dependency. In Section 4, we will compare estimates of future warming under the assumptions of independence and unknown dependency between model parameters.

2.4. Extending Belief Functions

For the application of p-boxes and belief functions to climate change assessments, we need a method to propagate these objects through dynamical models. Consider a model of some causal relationship, which generates a transfer function $f : \mathbb{R}^n \to \mathbb{R}^m$, $y = f(x)$. Let the uncertainty in the input variables x be described by $\Gamma_X(bel_\mathcal{E}) := \{ P_X \,|\, \forall\, A \in \mathcal{R}^n \;\; bel_\mathcal{E}(A) \leq P_X(A) \}$. The associated random set $(\mathcal{E}, m) = \{(E_1, m_1), ..., (E_k, m_k)\}$ can be transfered to the model output y by applying the so-called extension principle for random sets. It was introduced and named in analogy to the extension principle for fuzzy sets by Dubois and Prade [15], and is defined by

$$f(E_i) := \{ y \,|\, \exists\, x \in E_i \quad y = f(x) \} \, , \qquad m_f(B) := \sum_{f(E_i)=B} m_i \, . \tag{6}$$

We denote the transfered random set by $(f(\mathcal{E}), m_f)$, and the associated belief function by $bel_{f(\mathcal{E})}$.

The question remains whether extension (6) is a useful tool to transfer the convex set of probabilities $\Gamma_X(bel_\mathcal{E})$ to the model output space? Let the transfer function $f : \mathbb{R}^n \to \mathbb{R}^m$ be Borel measurable, i.e., $\forall\, B \in \mathcal{R}^m \;\; f^{-1}(B) = \{ x \in \mathbb{R}^n \,:\, f(x) \in B \} \in \mathcal{R}^n$. Then, every probability measure P_X on $(\mathbb{R}^n, \mathcal{R}^n)$ is transformed by the mapping f into a probability measure P_Y on $(\mathbb{R}^m, \mathcal{R}^m)$ defined by $\forall\, B \in \mathcal{R}^m \;\; P_Y(B) := P_X(f^{-1}(B))$. Using this definition, we can generate the transformed set of probabilities

$$f(\Gamma_X(bel_\mathcal{E})) := \{ P_Y \,|\, \exists\, P_X \in \Gamma_X(bel_\mathcal{E}) \;\; \forall\, B \in \mathcal{R}^m \;\; P_Y(B) = P_X(f^{-1}(B)) \} \, .$$

Thus, the question is how $f(\Gamma_X(bel_\mathcal{E}))$ relates to the set of probabilities $\Gamma_Y(bel_{f(\mathcal{E})})$ encompassed by the extended belief function $bel_{f(\mathcal{E})}$? To give a satisfactory answer, we need to know how to define a probability measure P_X from a probability P_Y on $\mathcal{R}^m$.

LEMMA 2. *Let $f : \mathbb{R}^n \to \mathbb{R}^m$ be a Borel measurable transfer function, whose range is a Borel set, i.e., $Rg(f) \in \mathcal{R}^m$. Let $\mathcal{F}$ be the collection of inverse images of the Borel sets, i.e., $\mathcal{F} := \{f^{-1}(B) \,|\, B \in \mathcal{R}^n \cap Rg(f)\}$. Define for each P_Y on $\mathcal{R}^m \cap Rg(f)$ a set function $P_{X|\mathcal{F}}$ on $\mathcal{F}$ by*

$$\forall\, A \in \mathcal{F} \;\; P_{X|\mathcal{F}}(A) := P_Y(f(A))\,. \quad \textit{Then,}$$

(a) $\mathcal{F}$ is a σ-field of subsets of $\mathbb{R}^n$ with $\mathcal{F} \subseteq \mathcal{R}^n$,
(b) the atoms of $\mathcal{F}$ are constituted by the sets $f^{-1}(y)$ with y in the range of f,
(c) $P_{X|\mathcal{F}}$ is a countably additive probability measure on $\mathcal{F}$.

Using the definition of $P_{X|\mathcal{F}}$ presented in Lemma 2, we can transform each element of $\Gamma_Y(bel_{f(\mathcal{E})})$ to a probability measure on $\mathcal{F}$, generating

$$f^{-1}(\Gamma_Y(bel_{f(\mathcal{E})})) := \\ \{\, P_{X|\mathcal{F}} \,|\, \exists\, P_Y \in \Gamma_Y(bel_{f(\mathcal{E})}) \;\; \forall\, A \in \mathcal{F} \;\; P_{X|\mathcal{F}}(A) = P_Y(f(A)) \,\}\,.$$

The following theorem shows that extension (6) yields indeed a belief function $bel_{f(\mathcal{E})}$ which describes the transformed set of probabilities $f(\Gamma_X(bel_{\mathcal{E}}))$ in a meaningful manner.

THEOREM 2. *Let $\mathcal{R}^n$, $\mathcal{R}^m$ be Borel fields, $f : \mathbb{R}^n \to \mathbb{R}^m$ a Borel measurable transfer function with $Rg(f) \in \mathcal{R}^m$.*

Let $bel_{\mathcal{E}}$ be a belief function, encompassing the set of probabilities $\Gamma_X(bel_{\mathcal{E}})$, and $(\mathcal{E}, m)$ the associated random set. Let

$$\Gamma_{X|\mathcal{F}}(bel_{\mathcal{E}}) := \{\, P_{X|\mathcal{F}} \,|\, \forall\, A \in \mathcal{F} \;\; P_{X|\mathcal{F}}(A) \geq bel_{\mathcal{E}}(A) \,\}$$

be the convex set of probabilities encompassed by the restriction of $bel_{\mathcal{E}}$ to $\mathcal{F}$.

Let $(f(\mathcal{E}), m_f)$ be the f-extension of $(\mathcal{E}, m)$ calculated from Equation (6), and $bel_{f(\mathcal{E})}$ the associated belief function. Let

$$\Gamma_Y(bel_{f(\mathcal{E})}) := \{\, P_Y \,|\, \forall\, B \in \mathcal{R}^m \quad bel_{f(\mathcal{E})}(B) \leq P_Y(B) \,\}\,.$$

Then,
(a) $f(\Gamma_X(bel_{\mathcal{E}})) \;\subseteq\; \Gamma_Y(bel_{f(\mathcal{E})})\,,$
(b) $\Gamma_{X|\mathcal{F}}(bel_{\mathcal{E}}) \;\supseteq\; f^{-1}(\Gamma_Y(bel_{f(\mathcal{E})}))\,.$

Theorem 2 shows that by applying the extension principle (6), we are not unwittingly adding information by excluding probabilities in $f(\Gamma_X(bel_{\mathcal{E}}))$ from the set of probabilities $\Gamma_Y(bel_{f(\mathcal{E})})$. Whether we might loose some information, i.e., $\Gamma_Y(bel_{f(\mathcal{E})}) \supset f(\Gamma_X(bel_{\mathcal{E}}))$, is more difficult to assess. No

information will be lost, if each probability measure $P_{X|\mathcal{F}} \in \Gamma_{X|\mathcal{F}}(bel_{\mathcal{E}})$ can be extended onto the larger Borel field $\mathcal{R}^n$ in a manner so that the extended probability P_X is contained in $\Gamma_X(bel_{\mathcal{E}})$. Whether this is possible, will depend on the type of transfer function f as well as belief function $bel_{\mathcal{E}}$. Fetz and Oberguggenberger [12] have shown that in any case

$$\inf_{P_Y \in f(\Gamma_X(bel_{\mathcal{E}}))} P_Y(B) = \inf_{P_Y \in \Gamma_Y(bel_{f(\mathcal{E})})} P_Y(B)$$

for arbitrary events $B \in \mathcal{R}^n$.

3. A Random Set for a Simple Climate Model

3.1. Global Mean Temperature Model

We use a simple dynamical model to calculate the response of global mean temperature (GMT) to a perturbation of the radiation balance between the incident solar radiation and the outgoing infrared radiation from the earth. The initial perturbation, excluding adjustments of the earth system, is expressed by an exogenous radiative forcing trajectory $Q(t)$ (in units of W m^{-2}). The temperature anomaly T specifies the global mean warming relative to the GMT value at preindustrial times (in units of °C).

$$C_e \cdot \dot{T}(t) = Q(t) - Q_{2x} \cdot \frac{T(t)}{T_{2x}} \,, \tag{7}$$

where
- C_e effective ocean heat capacity [J m^{-2} °C^{-1}] ,
- Q_{2x} rad. forcing from doubling atmospheric CO_2 [W m^{-2}] ,
- T_{2x} climate sensitivity [°C] .

Differential equation (7) is the simplest type of energy balance model, arising from a linear approximation of the change in the earth's energy balance for small perturbations [16]. It equates the net radiative flux into the system at the top of the atmosphere to surface heat uptake $C_e\dot{T}$, which is dominated by the ocean. If the radiative forcing were kept constant at a value $Q = Q_{2x}$, i.e., if the atmospheric CO_2 concentration is stabilized at twice its preindustrial value of 280 ppm, the system would undergo an equilibrium temperature change $T = T_{2x}$. *Climate sensitivity* T_{2x} is a crucial parameter to characterize the response of the climate system to an increase in GHG concentrations. Due to complex feedbacks, the value of climate sensitivity is clouded by uncertainty. Rising temperatures will increase the water vapor content in the atmosphere, which further enhances the absorption of infrared radiation from the surface, leading to an increase in

greenhouse forcing (*water vapor feedback*). Moreover, the planetary albedo, i.e., the overall reflectivity of the earth system to incident solar radiation, is likely to decrease due to, inter alia, changes in cloud cover, and a reduction in snow and ice cover (*albedo feedback*).

The Intergovernmental Panel on Climate Change (IPCC) gives an estimate of climate sensitivity $T_{2x} = [1.5\,^\circ\mathrm{C}, 4.5\,^\circ\mathrm{C}]$ based on the differences among state-of-the-art general circulation models [17]. The panel explicitly refrains from specifying probabilistic information. Recently, models of intermediate complexity were used to establish probability distributions from a comparison of model results with historical atmosphere, surface and deep ocean temperature data [18, 19, 20]. Efforts are hampered by the presence of natural variability, the lack of long-term data and the multitude of forcings.

In this analysis, we consider probability distributions for T_{2x} from two recent studies. Forest et al. [19] use Bayes' rule to update a prior for climate sensitivity with the likelihood that the historical data can be reproduced by the model. They specify two posterior distributions $P_{T_{2x}}$ for a uniform and an expert prior. Andronova and Schlesinger [20] use a bootstrapping method to determine various estimates of $P_{T_{2x}}$ for different assumptions about the radiative forcing from solar activity (S), volcanic sources, and tropospheric ozone (T). In their setup, they separate the stochastic uncertainty due to the presence of natural variability in the data from the epistemic uncertainty about the historical forcing trajectory. While the former is translated into a probability estimate for climate sensitivity, the latter uncertainty is dealt with by a sensitivity analysis. If we assume complete ignorance about whether solar activity and tropospheric ozone have contributed significantly to the temperature increase in the past, we can interpret the probability estimates $P(T_{2x})$ for solar and ozone forcing models included or excluded as extreme points of an imprecise probability.

The estimates for $P(T_{2x})$ are shown in Fig. 2. We construct a distribution band $\Gamma_{T_{2x}}(\underline{F}, \overline{F})$ by making two assumptions:

(A) *Inclusion of the plausible:* We assume that every CDF which lies between the lower and upper enveloping CDFs of the family of estimates is compatible with the current state of information.

(B) *Exclusion of the implausible:* We assume that every CDF which is not fully enclosed by the enveloping CDFs is not compatible with the current state of information.

Assumption (B) is rather reasonable, if the enveloping CDFs include all estimates that are "scientifically accepted"[2]. In this case, every estimate outside their range can be considered implausible until a scientific analysis

[2]We acknowledge that "scientifically accepted" is a difficult notion to work with, since it is both fuzzy and not necessarily related to truth. From a practical point of view,

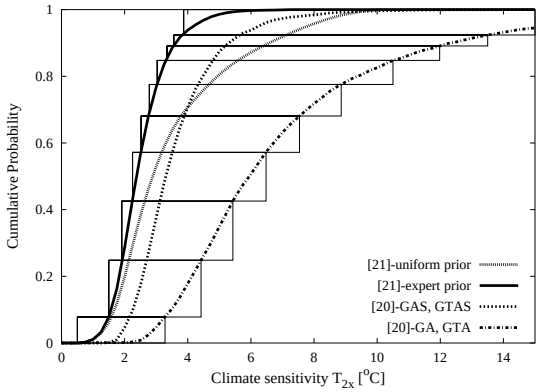

Figure 2. Cumulative probability distributions for T_{2x} from the literature [19, 20]: Estimates of [19] depend on a prior probability. Estimates of [20] depend on whether models for solar forcing (S), and tropospheric ozone (T) were considered in addition to greenhouse gas (G) and aerosol forcing (A) (specified by combinations of G, A, T, S). The distribution band $\Gamma_{T_{2x}}(\underline{F}, \overline{F})$ is enclosed by "[19]-expert prior" and "[20]-GA,GTA". Also shown are the p-box approximation and the associated random set.

has demonstrated the contrary. The situation is more difficult with Assumption (A). It basically says that every estimate should be considered plausible which cannot be excluded on the basis of Assumption (B). This is a very conservative statement, because we can imagine Dirac δ-measures with their masses concentrated at point values that look rather implausible, but are still fully enclosed by the enveloping CDFs.

The continuous distribution band $\Gamma_{T_{2x}}(\underline{F}, \overline{F})$ is bounded by "[19]-expert prior" from above and by "[20]-GA,GTA" from below. In order to generate a p-box $\Gamma_{T_{2x}}(\underline{SF}, \overline{SF})$, the continuous lower and upper bounds need to be approximated by step functions. Following [5], it is usually suggested to choose an equiprobable partition of the probability axis for generating lower and upper step functions that jump between these levels [4]. Depending on the application, however, other partitions might be better suited. In our case, it is desirable to minimize the additional imprecision introduced by the p-box approximation. This can be achieved by adjusting the step height of the approximating step functions to reflect the shape of the continuous bounding functions. If we use the area between lower and upper bounding function as an indicator for the degree of imprecision [11,

"scientifically accepted" could be defined as every estimate published in the literature and not considered outdated by the community. We do not claim to have included all such estimates in our analysis. The estimates we rely on were chosen for illustrative purposes.

Chap. 5], a partition of the probability axis into n levels that minimizes the degree of additional imprecision can be found by solving the following nonlinear program:

$$\max_{x_2^*,\ldots,x_n^*} \sum_{i=1}^{n} \left(\underline{F}(x_{*i}) - \overline{F}(x_i^*)\right) \cdot (x_{*i} - x_i^*) \ , \tag{8}$$

$$\text{subject to} \qquad \overline{F}(x_i^*) = \underline{F}(x_{*i-1}) \ , \quad x_i^* > x_{i-1}^* \ , \ \ 1 < i \leq n \ ,$$

where x_1^*, x_{*n} are fixed by the support $(x_1^*, x_{*n}]$ of the distribution band $\Gamma_X(\underline{F}, \overline{F})$. Note that knowledge of $x_2^*, ..., x_n^*$ fully determines $x_{*1}, ..., x_{*n-1}$ and the partition of the probability axis in intervals $[\overline{F}(x_{i+1}^*), \overline{F}(x_i^*)]\,, 1 \leq i < n$ and $[\overline{F}(x_n^*), 1]$. The resulting p-box $\Gamma_{T_{2x}}(\underline{SF}, \overline{SF})$ can be immediately decomposed into a random set

$$(\mathcal{E}, m) = \{\ (x_1^*, x_{*1}],\ m = \underline{F}(x_{*1});$$

$$(x_2^*, x_{*2}],\ m = \underline{F}(x_{*2}) - \overline{F}(x_2^*);\ ...;\ (x_n^*, x_{*n}],\ m = 1 - \underline{F}(x_n^*)\ \}\ . \tag{9}$$

We solved Program (8) for the distribution band $\Gamma_{T_{2x}}(\underline{F}, \overline{F})$ and the choice of $n = 10$ with the NLP solver CONOPT [21] in the General Algebraic Modeling System (GAMS) environment. CONOPT searches for a local optimum along the gradient of the objective function, which in our case is determined by the gradients of the lower and upper bounding functions. We varied the initial conditions to test for multiple local optima. The small number of $n = 10$ focal elements was chosen for illustration. Due to computational limitations, a random set for a more complex climate model will need to be restricted to a small number of focal elements.

Fig. 2 shows the resulting p-box $\Gamma_{T_{2x}}(\underline{SF}, \overline{SF})$ and its associated random set $(\mathcal{E}_{T_{2x}}, m)$. The information content of the p-box can be compared with the IPCC estimate of $T_x \in [1.5\,^\circ\text{C}, 4.5\,^\circ\text{C}]$ by drawing on the belief function representation of $\Gamma_{T_{2x}}(\underline{SF}, \overline{SF})$ that was established in Theorem 1. The lower probability $\underline{P}(T_{2x} \in [1.5\,^\circ\text{C}, 4.5\,^\circ\text{C}])$ and upper probability $\underline{P}(T_{2x} \in [1.5\,^\circ\text{C}, 4.5\,^\circ\text{C}])$, for instance, are given by

$$\begin{aligned} bel_{T_{2x}}(T_{2x} \in [1.5\,^\circ\text{C}, 4.5\,^\circ\text{C}]) &= \sum_{i \,|\, E_i \subseteq [1.5\,^\circ\text{C}, 4.5\,^\circ\text{C}]} m_i = 0.12 \ , \\ pl_{T_{2x}}(T_{2x} \in [1.5\,^\circ\text{C}, 4.5\,^\circ\text{C}]) &= \sum_{i \,|\, E_i \cap [1.5\,^\circ\text{C}, 4.5\,^\circ\text{C}] \neq \emptyset} m_i = 1 \ . \end{aligned}$$

By analogous calculations, the probability for $T_{2x} < 1.5\,^\circ\text{C}$ is found in the interval $[0, 0.08]$, and for $T_{2x} > 4.5\,^\circ\text{C}$ in $[0, 0.80]$. The numbers show that $\Gamma_{T_{2x}}(\underline{SF}, \overline{SF})$ does not support the IPCC estimate, especially for high climate sensitivities $T_{2x} > 4.5\,^\circ\text{C}$. This reflects the fact that the upper bound of the IPCC estimate is not supported by the probability estimates from the literature [19, 20] that we have considered here.

Climate sensitivity is not the only uncertain parameter in Equation (7). Effective ocean heat capacity C_e is an artificial quantity that arises from the simple form of the energy balance model. It depends on ocean characteristics like vertical diffusivity, but also on climate sensitivity [17]. A comparison of Model (7) with emulations of different general circulation models suggest a functional dependence of C_e on T_{2x} of the form $C_e \sim T_{2x}^{\gamma_c}$ with $0 < \gamma_c < 1$. We parameterize $C_e := \bar{C} \cdot (T_{2x}/3\,^\circ\mathrm{C})^{\gamma_c}$, where $\bar{C}$ specifies the effective heat capacity $\bar{C}$ for $T_{2x} = 3\,^\circ\mathrm{C}$. The uncertainty about C_e derives from the p-box for climate sensitivity, and the uncertainty about $\bar{C}$ and γ_c. We specify an interval uncertainty $(\bar{C}, \gamma_c) = [1.26\ \mathrm{GJ\ m^{-2}\,^\circ C^{-1}}, 1.58\ \mathrm{GJ\ m^{-2}\,^\circ C^{-1}}] \times [0.6,0.8]$ for the latter two parameters, which is an adequate choice in the light of the large uncertainty surrounding ocean characteristics like vertical diffusivity [19]. Interval uncertainty generates the simplest form of a p-box. The lower and upper CDF are either 0 or 1. Such a p-box can be captured by a random set containing just one focal element with probability mass $m = 1$.

3.2. Radiative Forcing Model

We group the radiation affecting substances into carbon dioxide, which is the most important GHG, the "other than CO_2" greenhouse gases (OGHGs), and aerosols. Solar and volcanic sources are neglected since we are interested in the human-induced climate change signal. The radiative forcing trajectory $Q(t)$ associated with the accumulation of these substances in the atmosphere relative to their preindustrial level is calculated by

$$Q(t) = \frac{Q_{2x}}{\ln 2} \ln\left(\frac{C_{CO_2}(t)}{C_{CO_2}(1750)}\right) + Q_{Aer}\, g(E_{Aer}(t)) + Q_{OGHG}(t)\ , \qquad (10)$$

where	C_{CO_2}	Atmospheric CO_2 concentration [ppm] ,
	E_{Aer}	Human sulfate aerosol emissions [TgS $\mathrm{yr^{-1}}$] ,
	Q_{Aer}	Net aerosol forcing in 1990 [W $\mathrm{m^{-2}}$] ,
	Q_{OGHG}	OGHG forcing trajectory [W $\mathrm{m^{-2}}$] .

The radiative properties of aerosol particles are most uncertain. Aerosols influence the radiation balance not only directly, but also indirectly by altering cloud formation processes. Both effects are included in the function $g(E_{Aer}(t))$, which employs a standard parametrization to convert aerosol emissions relative to their 1990 value to net aerosol radiative forcing relative to Q_{Aer} [16, Chap. 7.7]. The IPCC estimates that the negative forcing of aerosols has been in the range [-0.8 W $\mathrm{m^{-2}}$, -0.2 W $\mathrm{m^{-2}}$] (direct effect) and [-2 W $\mathrm{m^{-2}}$, 0 W $\mathrm{m^{-2}}$] (indirect effect) for the period 1990-2000 [22]. Forest et al. [19] and Andronova and Schlesinger [20] have also investigated the uncertainty about Q_{Aer}. Fig. 3 depicts their estimates for the

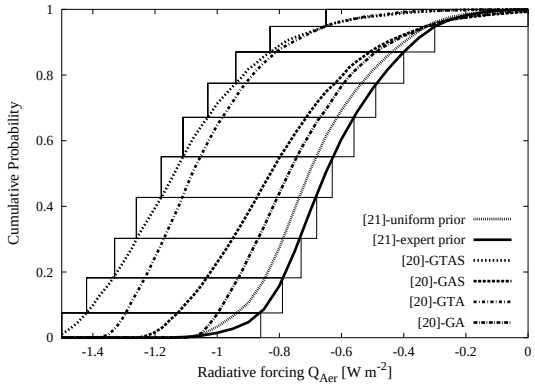

Figure 3. Cumulative probability distributions from the literature for Q_{Aer} [19, 20]. See Fig. 2 for additional explanation on the figure key. Also shown are the p-box approximation of the distribution band and the associated random set.

cumulative probability distribution of Q_{Aer} under different assumptions detailed in Section 3.1. As for climate sensitivity, we have used the lower and upper enveloping function of the family of estimates to construct a distribution band $\Gamma_{Q_{Aer}}(\underline{F}, \overline{F})$, and have solved Program (8) to determine a step function approximation for the choice of $n = 10$ steps.

The resulting p-box $\Gamma_{Q_{Aer}}(\underline{SF}, \overline{SF})$ and its associated random set are shown in Fig. 3. Their information content can be compared with the IPCC estimate [-2.8 W m^{-2}, -0.2 W m^{-2}] (direct and indirect effect combined). The probability $P(Q_{Aer} \in$ [-2.8 W m^{-2}, -0.2 W m^{-2}]) lies in the interval $[0.95, 1]$. Thus, the IPCC estimate includes $\Gamma_{Q_{Aer}}(\underline{SF}, \overline{SF})$ almost entirely. The estimates considered here support a more narrow range, where in particular a very strong negative aerosol forcing contribution is discarded.

We link the uncertainty in the time-dependent paths of atmospheric CO_2 concentration $C_{CO_2}(t)$, future changes in the radiative forcing of the OGHGs $Q_{OGHG}(t)$, and anthropogenic aerosol emissions $E_{Aer}(t)$ directly to the socio-economic sphere. In a special report on emissions scenarios [23], the IPCC has described a range of plausible future pathways of society and economy on a global scale. In this analysis, we specify just two parameters G ("growth") and S ("Shift"), with $C_{CO_2}(t) = C_{CO_2}(2000)\, e^{Gt - St^2}$, $Q_{OGHG}(t) = Q_{OGHG}(2000)\, e^{Gt - St^2}$ and $E_{Aer}(t) = E_{Aer}(2000)\, e^{Gt - (3S+D)t^2}$. We restrict $S \leq G/300$ years, so that the growth in atmospheric CO_2 concentration and radiative forcing of OGHGs can be dampened, but not reversed by a "shift" S in the 21st century. In contrast, aerosol emissions E_{Aer} will decrease eventually due to the presence of a desulphurization constant D in the exponent. This accounts for the fact

Focal elements for	T_{2x}	$\bar{C} \times \gamma_c$	Q_{Aer}	$G \times S$
Geometry	interval	rectangle	interval	triangle
Number	10	1	10	1

Table 1. List of uncertain model parameters and the properties of their associated random sets.

that aerosol emissions are projected to decline in the mid to long run due to increased local environmental protection.

As the future socio-economic development is entirely uncertain, it is appropriate to specify interval uncertainties for $G \in [\,0.004\,\mathrm{yr}^{-1},\, 0.012\,\mathrm{yr}^{-1}\,]$ and $S \in [\,0\,\mathrm{yr}^{-1},\, G/300\,\mathrm{yr}^{-2}\,]$. This defines a random set with a single triangular focal element on $\Omega_G \times \Omega_S$ carrying probability mass $m = 1$. Growth rates from 0.4% to 1.2% per year lead to atmospheric CO_2 concentrations from 480 ppm to 1230 ppm in 2100 (present day: 380 ppm), and to a forcing from the OGHGs between 1 and 4 W m^{-2}. This covers the full range of the scenarios including uncertainty in the biogeochemical cycles [17].

3.3. Joint Random Set for the Model Parameters

We have specified random sets for six uncertain parameters in the temperature model (7) and forcing model (10) (see Table 1). They can be associated with four physically distinct fields: climate feedbacks (T_{2x}), ocean properties ($\bar{C} \times \gamma_c$), aerosol properties (Q_{Aer}) and socio-economic behavior ($G \times S$). Hence, it is reasonable to assume physical independence between the parameters in the various fields. If we naively assume that this implies independence of the associated random sets, we can combine the random set information by applying the independent product (3). This generates a joint random set $(\mathcal{E}_{par}, m_{par})$, $par := (T_{2x},\, \bar{C},\, \gamma_c,\, Q_{Aer},\, G,\, S)$, with 100 focal elements $E_{i,par}$.

Consider the special case of complete ignorance over some domain Ω_1, which we have assumed for $\bar{C} \times \gamma_c$ and $G \times S$. It is captured by a p-box with lower CDF equal to zero and upper CDF equal to unity on Ω_1, and by a random set $(\mathcal{E}_1, m_1)$ with single focal element Ω_1. In this special case, the combination of $(\mathcal{E}_1, m_1)$ with some other random set on a domain Ω_2 yields the same result for the assumption of independence as for unknown dependency. Under both assumptions, the combination amounts to a mere extension of the Ω_2-random set onto the product space $\Omega_1 \times \Omega_2$. Thus, there exists a unique way to include the complete ignorance over $\bar{C} \times \gamma_c$ and $G \times S$ into the joint random set $(\mathcal{E}_{par}, m_{par})$, as long as no well-known dependencies between the parameters are postulated. The only critical case is the combination of the random sets for T_{2x} and Q_{Aer}.

Although T_{2x} and Q_{Aer} are physically independent, they are linked by our knowledge about the historical temperature record. Comparisons of

model results with historical data will have a tendency to produce high estimates of T_{2x} for a large negative radiative forcing Q_{Aer} of aerosols, and vice versa [19]. To account for this epistemic dependence, we have included a constraint in the analysis that rejects parameter combinations (T_{2x}, Q_{Aer}), if the weighted least-square sum of the residual between historical global mean temperature and model output becomes excessively large in terms of a χ^2-test. However, since the variance of natural temperature variability, as estimated from general circulation models [24], is of the order of magnitude of the residual, the constraint was not very restrictive. In future research, we will investigate how random sets can be constructed directly from a comparison of model output with data given some imprecise prior. For the time being, we stick with the independent product (3), and use the linear program with Constraints (4) and (5) to compare with the assumption of unknown dependency between T_{2x} and Q_{Aer}.

4. Estimation of Global Mean Temperature Change

Differential equation (7) and Radiative forcing model (10) generate a continuous transfer function $f : \mathbb{R}^6 \to \mathbb{R}$ that maps the uncertain model parameters to an increase T in GMT since 1860. We have used Extension (6) to transfer the random set $(\mathcal{E}_{par}, m)$ for the uncertain parameters to a random set $(\mathcal{E}_T, m)$ for GMT increase. This requires the calculation of the image $f(E_{i,par}) = [\underline{T}_i(t), \overline{T}_i(t)]$ [3] for each focal element in $(\mathcal{E}_{par}, m)$. After discretizing time into sufficiently small time steps Δt, the boundaries of the image $f(E_{i,par})$ at time $t_k = k\,\Delta t + t_0$ can be found by solving

$$\underline{T}_i(t_k) = \min_{(T_{2x},\bar{C},\gamma_c,Q_{Aer},G,S)\,\in\,E_{i,par}} T(t_k)\,, \tag{11}$$

$$\text{subject to} \quad T(t_l) = T(t_{l-1}) + \Delta t \cdot \left(\frac{Q(t_{l-1})}{C_e} - \frac{Q_{2x}}{C_e} \cdot \frac{T(t_{l-1})}{T_{2x}} \right)\,;$$

$$\overline{T}_i(t_k) = \max_{(T_{2x},\bar{C},\gamma_c,Q_{Aer},G,S)\,\in\,E_{i,par}} T(t_k)\,, \tag{12}$$

$$\text{subject to} \quad T(t_l) = T(t_{l-1}) + \Delta t \cdot \left(\frac{Q(t_{l-1})}{C_e} - \frac{Q_{2x}}{C_e} \cdot \frac{T(t_{l-1})}{T_{2x}} \right)\,.$$

We have solved Programs (11) and (12) for a choice of $\Delta t := 1$ yr, $t_0 = 1860$, and $k \in \{166, 191, 216, 241\}$ (years 2025, 2050, 2075, 2100) with the

[3] The extension of a half-closed interval through a continuous non-monotone transfer function can result in a half-closed or closed interval. To avoid unnecessary technicalities, we consider the convex hull of the extended focal elements. The clear distinction of half-closed and closed intervals was necessary to establish Theorem 1, but does not influence the results almost everywhere on the space of measurable events.

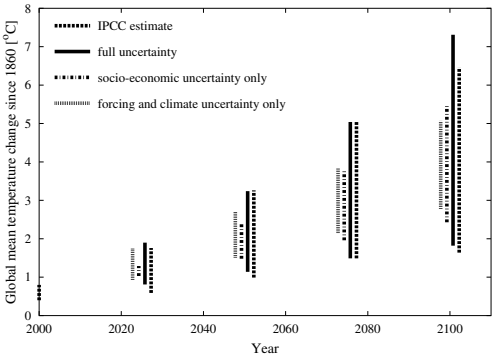

Figure 4. Image $[\underline{T}(t), \overline{T}(t)]$ of a single focal element [2.06 °C, 5.57 °C] × [-1.18 W m^{-2},-0.63 W m^{-2}] $\times(\bar{C}, \gamma_c, G, S) \in \mathcal{E}_{par}$ for the years 2025, 2050, 2075 and 2100. Shown are also the cases with solely socio-economic or solely forcing and climate uncertainty, and the IPCC estimate for the respective years.

NLP Solver CONOPT [21] in the GAMS environment. A historical forcing scenario was prescribed for the period 1860 to 2000.

It can be checked that $T(t)$ is monotone in $\bar{C}, \gamma_c, Q_{Aer}, G, S$ and concave in T_{2x}. The latter is due to the fact that T_{2x} influences T both directly and indirectly through its connection to effective ocean heat capacity. Thus, Program (12) is a convex optimization problem, and the solution will constitute the global maximum of temperature. Care has to be taken with Program (11). The solution will be a boundary point of the focal element $E_{i,par}$, and we have to check both boundary points to find the global minimum of T_{2x}.

Fig. 4 shows the image $[\underline{T}(t), \overline{T}(t)]$ of a single focal element. Its range grows considerably in time. We performed a sensitivity analysis with partly resolved uncertainty by assuming fixed average values for some parameters, while retaining the focal element for the other parameters (forcing and climate uncertainty: G, S fixed, socio-economic uncertainty: $T_{2x}, \bar{C}, \gamma^c, Q_{Aer}$ fixed). Uncertainty in the forcing and climate parameters dominates the overall uncertainty in the first half of the 21st century, but socio-economic uncertainty becomes equally important later on.

The transfered random set $(\mathcal{E}_T, m)$ for GMT increase can be used to construct a p-box $\Gamma_T(\underline{SF}, \overline{SF})$ with lower and upper bounding step functions

$$\underline{SF}(T) \quad := \quad bel_T(-\infty, T] = \sum_{i \mid E_{T,i} \subseteq (-\infty, T]} m_i \ , \tag{13}$$

$$\overline{SF}(T) \quad := \quad pl_T(-\infty, T] = \sum_{i \mid E_{T,i} \cap (-\infty, T] \neq \emptyset} m_i \ . \tag{14}$$

According to Corollary 1, the p-box $\Gamma_T(\underline{SF}, \overline{SF})$ contains the same or larger set of probabilities than is encompassed by the belief function bel_T, i.e., $\Gamma_T(bel_T) \subseteq \Gamma_T(\underline{SF}, \overline{SF})$. Equality holds if and only if $(\mathcal{E}_T, m)$ has Properties (I) and (II) in Lemma 1. However, due to the non-monotonicity of the dynamically generated transfer function, the extended random set $(\mathcal{E}_T, m)$ does not contain Property (II) any more, even though its inverse image did. Thus, $\Gamma_T(\underline{SF}, \overline{SF})$ contains less information than $\Gamma_T(bel_{\mathcal{E}})$ does. There are events $A \in \mathcal{R}$ for which $\underline{P}(A)$ calculated from $\Gamma_T(\underline{SF}, \overline{SF})$ is strictly smaller than $bel_T(A)$. We will give an example below.

For "well-behaved" transfer functions $y = f(x)$ [4], the following general relationship obtains when projecting a p-box for model parameters x onto the model output y:

$$f(\Gamma_X(\underline{SF}_X, \overline{SF}_X)) \overset{\text{Theorem 1}}{=} f(\Gamma_X(bel_X))$$

$$\overset{\text{Theorem 2}}{=} \Gamma_Y(bel_Y := f(bel_X)) \overset{\substack{\text{Corollary 1 \&} \\ \text{Non-monotone } f}}{\subset} \Gamma_Y(\underline{SF}_Y, \overline{SF}_Y) \; .$$

The information loss associated with the p-box $\Gamma_Y(\underline{SF}_Y, \overline{SF}_Y)$ will be the larger, the more non-monotone the transfer function is. Thus, bel_Y rather than $\Gamma_Y(\underline{SF}_Y, \overline{SF}_Y)$ should be used when determining lower and upper probabilities on the model output space. However, p-boxes are more illustrative to depict the resulting uncertainty for the model output variable.

Fig. 5 shows the lower and upper CDF of the p-box $\Gamma_T(\underline{SF}, \overline{SF})$ for the years 2025, 2050, 2075 and 2100. It can be seen that the imprecision in the GMT estimate is enormous (Fig. 5.a). A comparison with the IPCC estimate of [1.4 °C, 5.8 °C] for GMT increase in 2100 relative to 1990 [17] underscores this assessment. The probability for $T(2100) \in [1.6\,°\text{C}, 6.5\,°\text{C}]$ (assuming a warming of 0.2 °C to 0.7 °C until 1990) lies in the interval $[0, 1]$, for $T(2100) < 1.6\,°\text{C}$ in $[0, 0.23]$, and for $T(2100) > 6.5\,°\text{C}$ in $[0, 0.96]$. Despite the large range provided by the IPCC, the estimate of GMT increase presented here is too imprecise to discriminate against values outside this range. For the event $T(2100) \in [1.6\,°\text{C}, 6.5\,°\text{C}]$, the lower and upper probability calculated from bel_T do not differ from the values that can be derived from the p-box $\Gamma_T(\underline{SF}, \overline{SF})$. However, for the event $T(2100) \in [2.0\,°\text{C}, 7.3\,°\text{C}]$, e.g., it is $bel_T(T(2100) \in [2.0\,°\text{C}, 7.3\,°\text{C}]) = 0.16$, while the p-box allows for a lower probability of zero. This is one example for the loss of information discussed above.

[4] We call f well-behaved, if every probability measure $P_{X|\mathcal{F}}$ dominating the lower envelope bel_X of a p-box on the σ-field $\mathcal{F}$ can be extended to the Borel field $\mathcal{R}$ such that it dominates bel_X also on $\mathcal{R}$. If this is true, Theorem 2 establishes equality between the f-transformed p-box and the convex set of probabilities encompassed by the extended belief function bel_Y (see Section 2.4).

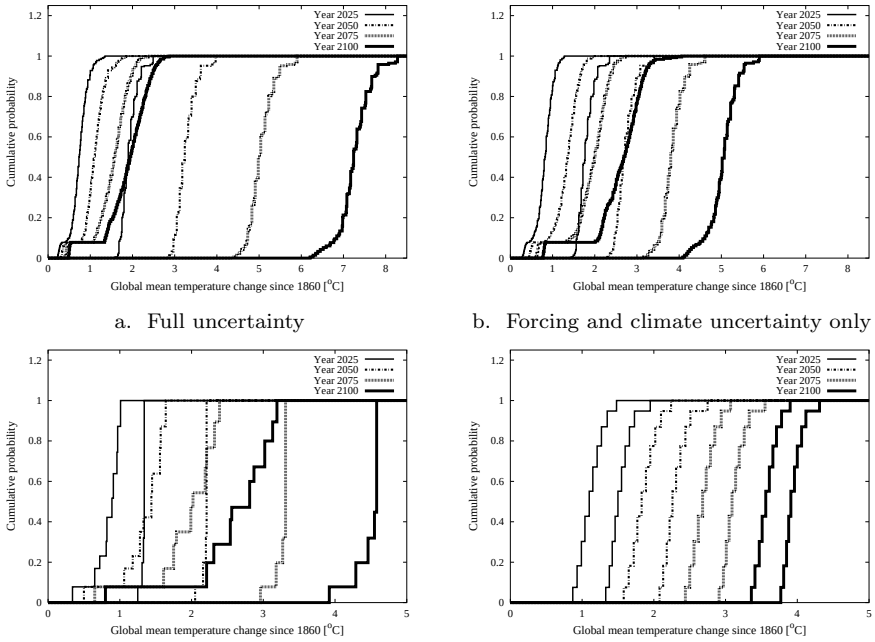

a. Full uncertainty

b. Forcing and climate uncertainty only

c. Climate uncertainty only

d. Forcing uncertainty only

Figure 5. Lower and upper CDFs for GMT increase T in the years 2025, 2050, 2075, 2100. Note the different scaling of the x-axis in c. and d.

The large imprecision is partly due to the large number of uncertain parameters that were captured by p-boxes describing complete ignorance $(\bar{C}, \gamma_c, G, S)$. The imprecision reduces considerably with the number of uncertain parameters. Fig. 5.b-d show cases, where we have fixed some parameters at an average value, while retaining the random set for the other parameters (forcing and climate uncertainty: G, S fixed; climate uncertainty: G, S, Q_{Aer} fixed; forcing uncertainty: $G, S, T_{2x}, \bar{C}, \gamma^c$ fixed). A comparison reveals that the socio-economic parameters are the most influential factor for the uncertainty in GMT increase in the year 2100, followed by the climatic parameters. The uncertainty about the aerosol forcing plays the smallest role, which is partly due to the fact that sulfate aerosol emissions are projected to certainly decline in the 21st century.

The imprecision in the estimate of future GMT change increases further, if we assume unknown dependency instead of independence between the random sets for T_{2x} and Q_{Aer}. Fig. 6 shows the difference between the p-box $\Gamma_T(\underline{SF}, \overline{SF})$ from Fig. 5 and the p-box that emerges when minimizing and maximizing cumulative probability for each event $(-\infty, T]$ under the constraints (4) and (5) for the allocation of probability masses over focal

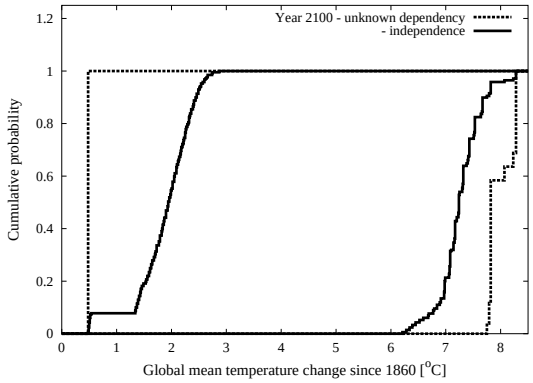

Figure 6. Lower and upper CDF for GMT increase T in the year 2100 under the assumption of independence and unknown dependency between T_{2x} and Q_{Aer}.

elements. The comparison reveals that the imprecision under independence is already large. It needs to be checked in further studies, in how far the imprecision decreases when a negative correlation between T_{2x} and Q_{Aer} is assumed.

5. Conclusion

Imprecise probability concepts carry the potential to consistently capture the different types of uncertainties and different degrees of knowledge that are encountered in climate change analysis. However, they need to be applicable to dynamical problems with a large number of uncertain continuous variables. We suggest that p-boxes and belief functions are conceptually flexible and mathematically tractable enough to fulfill these competing requirements to some extent. When a p-box is bounded by lower and upper step functions on the real line, the information about the encompassed set of probabilities can be condensed in a belief function and its associated random set. Moreover, if the random set extension principle is used to project a random set for model parameters onto the model output, no information is added unwittingly, i.e., no probabilities are excluded that were allowed under the initial uncertainty assessment.

We have constructed a belief function for a simple climate model, and projected it onto an estimate of global mean temperature increase. The large imprecision of the estimate has different reasons and implications. Firstly, we incorporated a very broad range of factors in the analysis. Imprecision will be reduced if the range of factors is limited by formulating

more specific questions. Secondly, we assumed a state of complete ignorance for two thirds of the parameters under consideration. Avoiding such crude estimates can greatly reduce imprecision. Thirdly, the p-boxes for T_{2x} and Q_{Aer} should be considered conservative estimates. They can be improved upon, when more comparisons of model results with historical data become available. Imprecision can be reduced in particular, if it is discriminated between the reliability of different models. Fourthly, we combined the marginal belief functions by assuming independence between T_{2x} and Q_{Aer}. The more appropriate assumption of a negative correlation between these two quantities would probably reduce imprecision.

Finally, one source of imprecision lies in the nature of the p-boxes themselves. They contain all Dirac δ-measures, whose CDF is encompassed by the lower and upper bounding functions. While it can be argued whether such degenerate probabilities should be included, they are having a large impact on processing the information, since they constitute the extreme points of the convex set of probabilities which set up the lower and upper envelope [25]. An alternative might be to consider probability families bounded by lower and upper probability density functions instead of p-boxes. However, such probability families are more general than belief functions, and cannot be represented like p-boxes (but a suitable approximation method has been proposed recently [26]).

Nevertheless, the results underline that uncertainty is a key issue in the integrated assessment of climate change. Belief functions provide new insights into the structure of the uncertainty, particularly into its imprecision. The link to p-boxes seems to be an important yardstick for assessing information losses when combining and extending belief functions. More work is needed here to enhance the applicability of belief functions to climate change analysis. We also need methods to determine belief functions directly from a comparison of model results with historical data.

Acknowledgments. We are grateful to Marco Zaffalon, Scott Ferson and one anonymous reviewer for many suggestions that helped to improve the paper. E.K. acknowledges support from the Deutsche Bundesstiftung Umwelt (German Federal Foundation of the Environment). Part of the work was conducted under a research grant of the VolkswagenStiftung.

6. APPENDIX

Proof of Lemma 1:

(I) Since at least one index $i \in \{1, ..., n\}$, $j \in \{1, ..., m\}$ is raised by one in each iteration, the algorithm enters step (2) at most $n + m - 1$ times before it stops.

(II) Since the indices $i \in \{1, ..., n\}$, $j \in \{1, ..., m\}$ are either raised by one or remain unchanged in each iteration, $i(k) \leq i(l)$ and $j(k) \leq j(l)$ for iterations $k < l$. Thus, $x^*_{j(k)} \leq x^*_{j(l)}$ and $x_{*i(k)} \leq x_{*i(l)}$ for iterations $k < l$.

(III) Consider an arbitrary $x \in \mathbb{R}$.
Belief function: If $x < x_{*1}$, then there exists no focal element with $E_k \subseteq (-\infty, x]$. Therefore, we have $bel(-\infty, x] = \underline{SF}(x) = 0$. If $x \geq x_{*n}$, then all focal elements have the property $E_k \subseteq (-\infty, x]$. Therefore, we have $bel(-\infty, x] = \underline{SF}(x) = 1$. Assume $x_{*1} \leq x < x_{*n}$. Let $E_l = (x^*_l, x_{*l}]$ be the focal element with $x_{*l} \leq x < x_{*l+1}$. Then, we have $bel_{\mathcal{E}}(-\infty, x] := \sum_{k|E_k \subseteq (-\infty, x]} m_k = \sum_{k \leq l} m_k$ due to (II). By construction of the algorithm, $\sum_{k \leq l} m_k = p_l := \underline{SF}(x_{*l})$. Since $x_{*l} \leq x < x_{*l+1}$, we have $\underline{SF}(x_{*l}) = \underline{SF}(x)$.

Plausibility function: If $x \leq x^*_1$, then all focal elements have the property $E_k \cap (-\infty, x] = \emptyset$. Therefore, we have $pl(-\infty, x] = \overline{SF}(x) = 0$. If $x > x^*_m$, then all focal elements have the property $E_k \cap (-\infty, x] \neq \emptyset$. Therefore, we have $pl(-\infty, x] = \overline{SF}(x) = 1$. Assume $x^*_1 < x \leq x^*_m$. Let $E_l = (x^*_l, x_{*l}]$ be the focal element with $x^*_l < x \leq x^*_{l+1}$. Then, we have $pl_{\mathcal{E}}(-\infty, x] := \sum_{k|E_k \cap (-\infty, x] \neq \emptyset} m_k = \sum_{k \leq l} m_k$ due to (II). By construction of the algorithm, $\sum_{k \leq l} m_k = p_l := \overline{SF}(x^*_{l+1})$. Since $x^*_l < x \leq x^*_{l+1}$, we have $\overline{SF}(x^*_{l+1}) = \overline{SF}(x)$. □

Proof of Theorem 1:

Step 1: The random set $\mathcal{E}$ has Property (III), Lemma 1. Hence, we have $\underline{P}_X(A) = bel_{\mathcal{E}}(A)$ for every event $A = (-\infty, x]$, $x \in \mathbb{R}$. Likewise, we have $\underline{P}_X(\emptyset) = bel_{\mathcal{E}}(\emptyset) = 0$, and $\underline{P}_X(\mathbb{R}) = bel_{\mathcal{E}}(\mathbb{R}) = 1$.

Step 2: Consider an arbitrary half closed interval $(a, b] \subset \mathbb{R}$, $a < b$. we have to show that $\underline{P}_X(a, b] = bel_{\mathcal{E}}(a, b]$.

$$\underline{P}_X(a, b] = \max[\,0, \underline{SF}(b) - \overline{SF}(a)] = \max[\,0, \sum_{i \mid E_i \subseteq (-\infty, b]} m_i - \sum_{j \mid E_j \cap (-\infty, a] \neq \emptyset} m_j\,].$$

If $\underline{SF}(b) < \overline{SF}(a)$, there exists a focal element $\hat{E} = (\hat{x}^*, \hat{x}_*] \in \mathcal{E}$ with $\hat{E} \cap (-\infty, a] \neq \emptyset$ and $\hat{E} \not\subseteq (-\infty, b]$. Assume now that an $\acute{E} \in \mathcal{E}$ with $\acute{E} = (\acute{x}^*, \acute{x}_*] \subseteq (a, b]$ would exist. Then, $a \leq \acute{x}^* < \acute{x}_* \leq b$, and $\hat{x}^* < \acute{x}^* < \acute{x}_* < \hat{x}_*$. The latter, however, contradicts Property (II) in Lemma 1, and we conclude that such an $\acute{E} \in \mathcal{E}$ does not exist. Hence, $bel_{\mathcal{E}}(a, b] = 0$.

Assume, vice versa, that there exists a focal element $\hat{E} \in \mathcal{E}$ with $\hat{E} \cap (-\infty, a] \neq \emptyset$ and $\hat{E} \not\subseteq -(\infty, b]$. Let E be an arbitrary focal element with $E \subseteq (-\infty, b]$. Then either $E \subseteq (a, b]$ or $E \cap (-\infty, a] \neq \emptyset$. It was shown in the last paragraph that the existence of $\hat{E}$ excludes $E \subseteq (a, b]$. Hence, all $E_i \subseteq (-\infty, b] \in \mathcal{E}$ intersect

$(-\infty, a]$, and $\underline{SF}(b) < \overline{SF}(a)$. Therefore, if $\underline{SF}(b) \geq \overline{SF}(a)$, there is no such focal element $\hat{E} \in \mathcal{E}$, i.e., for all focal elements $E_i \not\subseteq (-\infty, b] \Rightarrow E_i \cap (-\infty, a] = \emptyset$. Then,

$$\underline{P}_X(a,b] = \sum_{E_{s(i)} \subseteq (a,b]} m_{s(i)} + \sum_{E_{t(i)} \cap (-\infty,a] \neq \emptyset} m_{t(i)} - \sum_{E_j \cap (-\infty,a] \neq \emptyset} m_j = bel_{\mathcal{E}}(a,b] \; .$$

Step 3: Consider an arbitrary Borel set $B \in \mathcal{R}$. Let $E_1, ..., E_n$ be the focal elements that are fully contained in B, and $E_{n+1}, ...E_k$ the remaining focal elements of $\mathcal{E}$. Due to Lemma 1, Property (I), $E = \cup_{i=1}^{n} E_i$ is a union of $m \leq n$ disjoint half-closed intervals $E = (a_1, b_1] \cup ... \cup (a_m, b_m]$, $a_1 < b_1 < ... < a_m < b_m$, where no pair of half-closed intervals exhibits common accumulation points. Choose a CDF $F' : \mathbb{R} \to [0,1]$ with $F'(a_1) = \min[\overline{SF}(a_1), \underline{SF}(b_1)]$, $F'(b_1) = \underline{SF}(b_1)$, ..., $F'(a_m) = \min[\overline{SF}(a_m), \underline{SF}(b_m)]$, $F'(b_m) = \underline{SF}(b_m)$. Since $F'(a_1) \leq F'(b_1) \leq ... \leq F'(a_m) \leq F'(b_m)$, such a CDF does exist, and is contained in $\Gamma_X(\underline{SF}, \overline{SF})$. Given this probability specification, we have

$$\begin{aligned} P'(E) &= F'(b_m) - F'(a_m) + ... + F'(b_1) - F'(a_1) \\ &= \max[0, \underline{SF}(b_m) - \overline{SF}(a_m)] + ... + \max[0, \underline{SF}(b_1) - \overline{SF}(a_1)] \\ &= \underline{P}_X(a_m, b_m] + ... + \underline{P}_X(a_1, b_1] \; . \end{aligned}$$

Since the lower envelope $\underline{P}_X$ is super-additive on a union of disjoint sets [11, Ch. 2.7.4], we have $\underline{P}_X(E) = P'(E)$. Since $\underline{P}_X(a_i, b_i] = bel(a_i, b_i]$ as shown in Step 2, and each focal element contained in E is contained in exactly one interval $(a_i, b_i]$,

$$\underline{P}_X(E) \;=\; \sum_{i=1}^{l} \sum_{j | E_j \subseteq (a_i, b_i]} m_j \;=\; \sum_{j | E_j \subseteq \bigcup_{i=1}^{k} (a_i, b_i]} m_j \;=\; bel_{\mathcal{E}}(E) \; .$$

Since a lower envelope $\underline{P}_X$ is a monotone set function, we have

$$\underline{P}_X(B) \;\geq\; \underline{P}_X(E) \;=\; bel_{\mathcal{E}}(E) \;=\; bel_{\mathcal{E}}(B) \; .$$

Step 4: Consider an arbitrary Borel set $B \in \mathcal{R}$. Let $E_1, ..., E_n$ be the focal elements that are fully contained in B, and $E_{n+1}, ..., E_k$ the remaining focal elements of $\mathcal{E}$. Choose a right-continuous step function $SF^* : \mathbb{R} \to [0,1]$ as follows. For each focal element $E_i \not\subseteq B$, $n < i \leq k$, introduce a step of height m_i at a point $x_i \in E_i$, $x_i \notin B$. For each focal element $E_i \subseteq B$, $1 \leq i \leq n$ introduce a step of height m_i at an arbitrary point $x_i \in E_i$. Since $\sum_{i=1}^{k} m_i = 1$, SF^* so defined is a CDF of some Dirac δ-measure P^*. Moreover, we have

$$\begin{aligned} \forall\, x \in \mathbb{R} \quad SF^*(x) &\geq \sum_{j \;|\; E_j \subseteq (-\infty, x]} m_j = bel(-\infty, x] = \underline{SF}(x) \; , \\ SF^*(x) &\leq \sum_{j \;|\; E_j \cap (-\infty, x] \neq \emptyset} m_j = pl(-\infty, x] = \overline{SF}(x) \; , \end{aligned}$$

so that $P^* \in \Gamma_X(\underline{SF}, \overline{SF})$. Clearly, $P^*(B) = \sum_{i=1}^{n} m_i = \sum_{i \mid E_i \subseteq B} m_i = bel_{\mathcal{E}}(B)$. Since we have established $\underline{P}_X(B) \geq bel_{\mathcal{E}}(B)$ for arbitrary Borel sets B in Step 3, it is $\underline{P}_X(B) = bel_{\mathcal{E}}(B)$. □

Proof of Corollary 1:

Show $\boldsymbol{\Gamma_X(bel_{\mathcal{E}}) \subseteq \Gamma_X(\underline{SF}, \overline{SF})}$:
Choose an arbitrary probability $P_X \in \Gamma_X(bel_{\mathcal{E}})$.
$\Rightarrow \quad \forall\, x \in \mathbb{R} \;\; P_X(-\infty, x] \geq bel_{\mathcal{E}}(-\infty, x] \leq$ and $P_X(-\infty, x] \leq pl_{\mathcal{E}}(-\infty, x]$.
$\Rightarrow P_X \in \Gamma_X(\underline{SF}, \overline{SF})$ by definition.

Show $\boldsymbol{\Gamma_X(bel_{\mathcal{E}}) = \Gamma_X(\underline{SF}, \overline{SF})}$, if $\boldsymbol{(\mathcal{E}, m)}$ has Properties (I) and (II):
Use Algorithm 1 to construct a random set $(\mathcal{E}', m')$ from $\underline{SF}$ and $\overline{SF}$. $(\mathcal{E}', m')$ and $(\mathcal{E}, m)$ both have Properties (I) to (III), Lemma 1. This implies, inter alia, that for any half-closed interval $(a, b]$ on the real line we have $bel_{\mathcal{E}'} = bel_{\mathcal{E}} := \max[0, \underline{SF}(b) - \overline{SF}(a)]$ (see Step 1 in Proof of Theorem 1). Since both random sets contain only half-closed intervals, it follows $(\mathcal{E}', m') = (\mathcal{E}, m)$. Hence, $bel_{\mathcal{E}} = bel_{\mathcal{E}'}$, and according to Theorem 1, $bel_{\mathcal{E}}$ is the lower envelope of $\Gamma_X(\underline{SF}, \overline{SF})$.

Show $\boldsymbol{\Gamma_X(bel_{\mathcal{E}}) = \Gamma_X(\underline{SF}, \overline{SF})}$, only if $\boldsymbol{(\mathcal{E}, m)}$ has Properties (I), (II):
Assume that $(\mathcal{E}, m)$ does not fulfill property (I) or (II) in Lemma 1. Let $(\mathcal{E}', m')$ be the random set constructed from $\underline{SF}$, and $\overline{SF}$ by Algorithm 1, and $bel_{\mathcal{E}'}$ the associated belief function. According to Lemma 1, $(\mathcal{E}', m')$ has properties (I) to (II). Then, $(\mathcal{E}, m) \neq (\mathcal{E}', m')$, and $bel'_{\mathcal{E}} \neq bel_{\mathcal{E}}$. According to Theorem 1, $bel'_{\mathcal{E}}$ is the lower envelope of $\Gamma_X(\underline{SF}, \overline{SF})$. Hence, $bel_{\mathcal{E}}$ cannot be the lower envelope, and $\Gamma_X(bel_{\mathcal{E}}) \neq \Gamma_X(\underline{SF}, \overline{SF})$. □

Proof of Lemma 2:

The following properties hold in general for inverse images $f^{-1}(B) = \{x \mid f(x) \in B\}$ [6, Appendix A7]: $f^{-1}(\cup_\theta B_\theta) = \cup_\theta f^{-1}(B_\theta)$, $f^{-1}(\cap_\theta B_\theta) = \cap_\theta f^{-1}(B_\theta)$ for arbitrary (possibly uncountable) unions and intersections, and $B_1 \cap B_2 = \emptyset \;\Rightarrow\; f^{-1}(B_1) \cap f^{-1}(B_2) = \emptyset$.

Part (a): $\mathcal{F} \subseteq \mathcal{R}^n$ follows from the definition of $\mathcal{F}$, the measurability of f and the fact that $\mathrm{Rg}(f)$ is a Borel set. $\mathcal{F}$ is a σ-field on $\mathbb{R}^n$, if

1. $\mathbb{R}^n \in \mathcal{F}$: True, since $\mathbb{R}^n = f^{-1}(\mathrm{Rg}(f))$ and $\mathrm{Rg}(f) \in \mathcal{R}^m \cap \mathrm{Rg}(f)$.
2. $A \in \mathcal{F} \;\Rightarrow\; A^c \in \mathcal{F}$: Consider an arbitrary $A \in \mathcal{F}$. By definition of $\mathcal{F}$, it exists $B \in \mathcal{R}^m \cap \mathrm{Rg}(f)$ with $A = f^{-1}(B)$. Define $B' = \mathrm{Rg}(f) - B$. It is $f^{-1}(B \cup B') = f^{-1}(B) \cup f^{-1}(B') = A \cup f^{-1}(B')$. Since $B \cap B' = \emptyset$, $A \cap f^{-1}(B') = \emptyset$. Since $f^{-1}(B \cup B') = \mathbb{R}^n$, $A^c = f^{-1}(B')$. Thus, $A^c \in \mathcal{F}$.
3. For any collection $A_i \in \mathcal{F}$, it is $\cup_i A_i \in \mathcal{F}$: For each A_i in $\mathcal{F}$, it exists $B_i \in \mathcal{R}^m \cap \mathrm{Rg}(f)$ with $A_i = f^{-1}(B_i)$. Thus, $\cup_i A_i = \cup_i f^{-1}(B_i) = f^{-1}(\cup_i B_i)$. Since for any collection $B_i \in \mathcal{R}^m \cap \mathrm{Rg}(f)$ it is also $\cup_i B_i \in \mathcal{R}^m \cap \mathrm{Rg}(f)$, we have $\cup_i A_i \in \mathcal{F}$.

Part (b): $\{f^{-1}(y) \mid y \in \mathrm{Rg}(f)\}$ is the set of atoms of $\mathcal{F}$, if

1. $f^{-1}(y) \cap f^{-1}(y') = \emptyset$ for $y \neq y'$: True, since $\{y\} \cap \{y'\} = \emptyset$, if $y \neq y'$.
2. For all $A \in \mathcal{F}$, there exists a set $B \in \mathcal{P}(\mathbb{R}^m) \cap \mathrm{Rg}(f)$ with $A = \cup_{y \in B} f^{-1}(y)$: True, since by definition of $\mathcal{F}$, there exists a set $B \in \mathcal{R}^m \cap \mathrm{Rg}(f)$ for all $A \in \mathcal{F}$ with $A = f^{-1}(B) = f^{-1}(\cup_{y \in B} y) = \cup_{y \in B} f^{-1}(y)$.

Part (c): Note that $P_{X|\mathcal{F}}(A) := P_Y(f(A))$ is always defined on $\mathcal{F}$, since $\mathrm{Rg}(f)$ is a Borel set, and $\forall\, A \in \mathcal{F}\ \ f(A) \in \mathcal{R}^m \cap \mathrm{Rg}(f)$ by definition of $\mathcal{F}$. $P_{X|\mathcal{F}}$ is a countably additive probability measure on $\mathcal{F}$, if

1. For all $A \in \mathcal{F}\ \ P_{X|\mathcal{F}}(A) \geq 0$: True, by definition of $P_{X|\mathcal{F}}$, and the fact that P_Y is a probability measure.
2. $P_{X|\mathcal{F}}(\mathbb{R}^n) = 1$: True, since $f(\mathbb{R}^n) = \mathrm{Rg}(f)$ is a Borel set, and $P_Y(\mathrm{Rg}(f)) = 1$.
3. For any collection $A_i \in \mathcal{F}$ with $A_i \cap A_j = \emptyset$ for $i \neq j$, it is $P_{X|\mathcal{F}}(\cup_i A_i) = \sum_i P_{X|\mathcal{F}}(A_i)$:
   We have $P_{X|\mathcal{F}}(\cup_i A_i) := P_Y(f(\cup_i A_i)) = P_Y(\cup_i f(A_i))$. It follows from Part (b) that $A_i = f^{-1}(f(A_i))$. Hence, we have $A_i = f^{-1}(\cup_{y \in f(A_i)} y) = \cup_{y \in f(A_i)} f^{-1}(y)$. Then, $A_i \cap A_j = \emptyset$ for $i \neq j$ implies $f(A_i) \cap f(A_j) = \emptyset$ for $i \neq j$. Thus, $P_Y(\cup_i f(A_i)) = \sum_i P_Y(f(A_i)) =: \sum_i P_{X|\mathcal{F}}(A_i)$, since P_Y is a countably additive probability measure. $\square$

Proof of Theorem 2:

Part (a): Consider an arbitrary probability $P_Y \in f(\Gamma_X(bel_{\mathcal{E}}))$. There exists a probability $P_X \in \Gamma_X(bel_{\mathcal{E}})$ with $P_Y(B) = P_X(f^{-1}(B))$ for all $B \in \mathcal{R}^m$. For arbitrary $B \in \mathcal{R}^m$, we have

$$\begin{aligned} P_Y(B) &= P_X(f^{-1}(B)) \geq bel_{\mathcal{E}}(f^{-1}(B)) = \sum_{E_i \subseteq f^{-1}(B)} m_i \\ &= \sum_{f(E_i) \subseteq B} m_i = bel_{f(\mathcal{E})}(B)\,. \quad \text{Thus, } P_Y \in \Gamma_Y(bel_{f(\mathcal{E})})\,. \end{aligned}$$

Part (b): Consider an arbitrary probability $P_{X|\mathcal{F}} \in f^{-1}(\Gamma_Y(bel_{f(\mathcal{E})}))$. There exists a probability $P_Y \in \Gamma_Y(bel_{f(\mathcal{E})})$ with $P_{X|\mathcal{F}}(A) = P_Y(f(A))$ for all $A \in \mathcal{F}$. For arbitrary $A \in \mathcal{F}$, we have

$$\begin{aligned} P_{X|\mathcal{F}}(A) = P_Y(f(A)) \geq bel_{f(\mathcal{E})}(f(A)) &= \sum_{f(E_i) \subseteq f(A)} m_i \\ &= \sum_{E_i \subseteq f^{-1}(f(A))} m_i = bel_{\mathcal{E}}(A)\,, \end{aligned}$$

since $\mathcal{F}\ \ A = f^{-1}(f(A))$ by definition of $\mathcal{F}$. Thus, $P_{X|\mathcal{F}} \in \Gamma_{X|\mathcal{F}}(bel_{\mathcal{E}})$. $\square$

References

1. W. Luo, W. F. Caselton, Using Dempster-Shafer theory to repesent climate change uncertainties, Journal of Environmental Management 49 (1997) 73–93.
2. A. P. Dempster, Upper and lower probabilities induced by a multivalued mapping, Ann. Math. Statist. 38 (1967) 325–339.
3. S. Basu, A. DasGupta, Bayesian analysis under distribution bands, Tech. Rep. 90–48, Department of Statistics, Purdue University (1990).
4. S. Ferson, L. R. G. V. Kreinovich, D. S. Myers, K. Sentz, Constructing probability boxes and Dempster-Shafer structures, Tech. Rep. SAND2002-4015, Sandia National Laboratories, Albuquerque, NM (2003).
URL `www.sandia.gov/epistemic/Reports/SAND2002-4015.pdf`
5. R. C. Williamson, T. Downs, Probabilistic arithmetic I: numerical methods for calculating convolutions and dependency bounds, International Journal of Approximate Reasoning 4 (1990) 89–158.
6. P. Billingsley, Probability and Measure, Wiley Interscience, New York, 3rd edition, 1995.
7. G. Shafer, A Mathematical Theory of Evidence, Princeton U. Press, Princeton, 1976.
8. R. R. Yager, Arithmetic and other operations on Dempster-Shafer structures, International Journal of Man-Machine Studies 25 (1986) 357–366.
9. H. M. Regan, S. Ferson, D. Berleant, Equivalence of methods for uncertainty propagation of real-valued random variables, International Journal of Approximate Reasoning 36 (2004) 1–30.
10. I. Couso, S. Moral, P. Walley, A survey of concepts of independence for imprecise probabilities, Risk, Decision and Policy 5 (2000) 165–181.
11. P. Walley, Statistical Reasoning with Imprecise Probabilities, Chapman and Hall, London, 1991.
12. T. Fetz, M. Oberguggenberger, Propagation of uncertainty through multivariate functions in the framework of sets of probability measures, Reliability Engineering and System Safety 85 (2004) 73–87.
13. G. de Cooman, Random set independence is weaker than epistemic irrelevance, Personal communication (2004).
14. D. Berleant, J. Zhang, Representation and problem solving with the distribution envelope determination (DEnv) method, Reliability Engineering and System Safety 85 (2004) 153–168.
15. D. Dubois, H. Prade, Random sets and fuzzy interval analysis, Fuzzy Sets and Systems 42 (1991) 87–101.
16. L. D. D. Harvey, Global Warming: The Hard Science, Prentice Hall, Harlow, 2000.

17. U. Cubasch, G. Meehl, Projections of future climate change, in: J. Houghton, Y. Ding (Eds.), Climate Change 2001: The Scientific Basis, Cambridge University Press, Cambridge, 2001, pp. 525–582.

18. R. Knutti, T. F. Stocker, F. Joos, G. K. Plattner, Constraints on radiative forcing and future climate change from observations and climate model ensembles, Nature 416 (2002) 719–723.

19. C. E. Forest, P. H. Stone, A. P. Sokolow, M. R. Allen, M. D. Webster, Quantifying uncertainties in climate system properties with the use of recent climate observations, Science 295 (2002) 113–117.

20. N. G. Andronova, M. E. Schlesinger, Objective estimation of the probability density function for climate sensitivity, Journal of Geophysical Research 106 (2001) 22605–22611.

21. A. S. Drud, CONOPT: A large-scale GRG code, ORSA Journal on Computing 6 (1992) 207–216.

22. V. Ramaswamy, Radiative forcing of climate change, in: J. Houghton, Y. Ding (Eds.), Climate Change 2001: The Scientific Basis, Cambridge University Press, Cambridge, 2001, pp. 289–348.

23. N. Nakićenović, R. Swart, Emissions Scenarios. Special Report of the IPCC, Cambridge University Press, Cambridge, 2000.

24. M. Collins, S. F. B. Tett, C. Cooper, The internal climate variability of HadCM3, a version of the Hadley Centre coupled model without flux adjustments, Climate Dynamics 17 (2001) 61–81.

25. I. Kozine, V. Krymsky, Reducing uncertainty by imprecise judgements on probability distributions: Application to system reliability, in: Proceedings of the Third International Symposium on Imprecise Probabilities and Their Applications, 2003, pp. 335–344.

26. J. Hall, J. Lawry, Generation, combination and extension of random set approximations to coherent lower and upper probabilities, Reliability Engineering and System Safety 85 (2004) 89–101.